Internet Electronic Journal*

Nanociencia et Moletrónica

Diciembre 2008, Vol. 6, N°2, pp. 1247-1262

Parameter Adjustment of Active Models for Contour Detection with Application in AFM Images

J. N. Hwang[1], M. A. Torres-Tello[2], R. Rosas-Romero[2], O. Starostenko[2], V. Alarcón-Aquino[2], J. Rodríguez-Asomoza[2]

[1]Department of Electrical Engineering,
University of Washington, Seattle, Washington, **U. S. A.**
[2]CENTIA Research Laboratory, Computer Science Department,
Universidad de las Americas Puebla, Puebla, **Mexico**
e-mail: roberto.rosasudlap.mx

recibido: 01.11.08 revisado: 02.12.08 publicado: 31.12.08

Citation of the article;
J. N. Hwang, M. A. Torres-Tello, R. Rosas-Romero, O. Starostenko, V. Alarcón-Aquino, J. Rodríguez-Asomoza, Parameter Adjustment of Active Models for Contour Detection with Application in AFM Images Internet Electron. J. Nanoc. Moletrón. 2008, Vol.6, N°2, pp 1247-1262

Parameter Adjustment of Active Models for Contour Detection with Application in AFM Images

J. N. Hwang[1], M. A. Torres-Tello[2], R. Rosas-Romero[2], O. Starostenko[2], V. Alarcón-Aquino[2], J. Rodríguez-Asomoza[2]

[1]Department of Electrical Engineering,
University of Washington, Seattle, Washington, **U. S. A.**
[2]CENTIA Research Laboratory, Computer Science Department,
Universidad de las Americas Puebla, Puebla, **Mexico**
e-mail: roberto.rosasudlap.mx

recibido: 01.11.08 revisado: 02.12.08 publicado: 31.12.08

Internet Electron. J. Nanoc. Moletrón., Vol. 6, N° 2, pp. 1247-1262

Abstract

In the area of digital image processing, active models or snakes are mainly used for detection of object contours such as those in AFM images (Atomic Force Microscope), with certain characteristics defined by the user using prior knowledge. This information is utilized for object segmentation, object tracking, object recognition and other tasks. In this report an analysis of the main characteristics of three parametric active models (Kass, Cohen and Xu) is done. A comparative table is shown to help the user to define which could be the best model according to the application. Finally an experimental design is used to adjust the parameters of the models to guarantee a desired out put. Due to the fact that under some environments some active contour models can be recognized as being the most suitable for application, the relation among the three most referenced parametric active contour models and the selection of parameter values for each model is required for complex applications. Parameter selection is a general problem that is continuously commented in the references of this paper, and that is why a new alternative was developed to find the best parameters by means of experimentation.

1. Introduction

In 1987, William Kass [1] and his colleges proposed a new way to detect certain characteristics of objects in an image through a low level image process. They created a model that due to its characteristics was called *active model* or *snake*. Active models are based on *prior knowledge* [2] that can be defined as that knowledge or features of interest that are integrated on the model prior its implementation giving in this way more flexibility to the user. Besides prior knowledge, the possibility to find more than one solution gives more versatility to the model if it is compared to those low image process methods as *filters* or *templates* [2]. An example of an AFM image where contour detection is applied is shown in Figure 1.

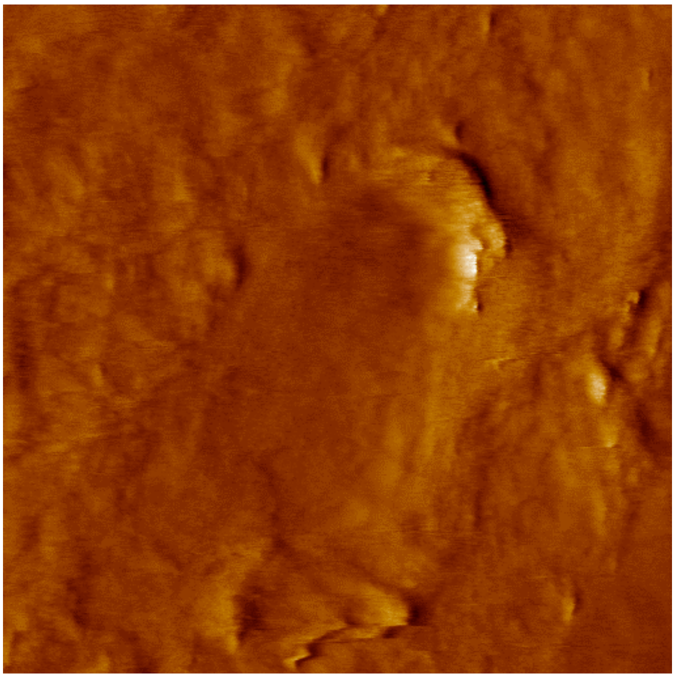

Fig. 1. AFM Image* (JSPM-5200) in $CuInSe_2$ Contact Force Mode

Although the active model of Kass represents a useful tool for detection of edges, lines or contours, it has been shown [3] that it lacks convergence to the desired solution under certain situations, i.e., far initialization of control points. Therefore, other models have been developed in order to solve the disadvantages of the original. Two alternatives were chosen in this project; the models of Laurent Cohen [4] and of Chenyang Xu [5]. They were chosen due to their applications and their facility to be programmed. It is important to say that all the models studied in this report are known [6] more specifically as *snaxels* that are part of the parametric active models. This name is given because the model is formed by a set of discrete control points.

One negative feature of any active model is that every characteristic used for prior knowledge must be regularized by a parameter that, in consequence, takes off generality. Some solutions to find good values for the parameters have been defined using design of experiments [7]. In this report, a precise output is defined in order to get adequate parameters. Unfortunately this method is not optimum and it is in some cases slow. Nevertheless, it will ensure a good result depending on the outputs of the experiment. An application example will be shown in this report using the design of experiments to fix the values of the parameters and a correct model according to the analysis of the three models. A conclusion of this work is done at the end of this report and possibilities for future work in this field are proposed.

2. Kass model

The Kass model is defined as a parametric curve that is moving through a spatial domain guided by the result of minimizing a functional [1]. This section will study every important term in the previous definition in order to get the main idea of the active model.

3. Parametric active models

A parametric active model can be represented mathematically as a curve $\mathbf{v}(s)=[x(s),y(s)]$ that is constantly moving in space (the image) over a number of iterations that could be interpreted as a sequence of time. In this curve the parameter is represented by s where $s\in[0,1]$. There is another parameter *t* related to the number of iterations. The parameter *s* is considered in this analysis only without loosing generality.

The curve $\mathbf{v}(s)$ must find certain characteristics defined by the user (prior knowledge) having also an intrinsic characteristics that will keep the correct shape of the curve. This problem could be solved through a differential equation that ensures a minimum in a functional (a function that depends of other functions), let say E^*_{snake} that is defined by the following equation

$$E^*_{snake}=\int_0^1 E_{snake}(\mathbf{v}(s)) \tag{1}$$

The energy functional E_{snake} in (1) has properties that the user defines and also controls the internal behavior of the active model. This energy functional can be expressed as follows

$$E_{snake}(v(s))=E_{intern}(v(s))+E_{image}(v(s))+E_{extern\_force}(v(s)) \tag{2}$$

where the energy functional $E_{intern}(\mathbf{v}(s))$ is defined by the following equation

$$E_{intern}(\mathbf{v}(s)) = \frac{1}{2}\alpha\,|\mathbf{v}_s(s)|^2 + \frac{1}{2}\beta\,|\mathbf{v}_{ss}(s)|^2 \tag{3}$$

where subscript *s* represents derivatives with respect to *s* and the number of subscripts represents the derivative order. Also it is considered in equation (3) that α(*s*) = α and β(*s*) = β. These variables are forced to be constants to simplify the model.

Equation (3) has two terms that could be related to the physical behavior of a spring. If it is considered to have a measure of the arc length of the curve and that equation (2) is minimized, then the active contour collapses. The first term in equation (3) is also known as tension term. The term *tension* is given to α due to the fact that the first order derivative $\mathbf{v}_s(s)$ has “big values” on discontinuities or holes in the curve. The second term in (3) represents changing rates of the tangent by the term $\mathbf{v}_{ss}(s)$ in (3). As previously mentioned, at the beginning of this section, it is necessary to find an expression for the curve that generates minimums for the energy functional that will be reached on the desired characteristics. Therefore, any expression that reaches high values is a behavior or characteristic that is not desired in the model. That is, in (3) the model promotes unity of the control points (low discontinuities) and smoothness (low variance of the tangent changing rate). The first is known as the elasticity property and the second as the rigidity property [1, 2].
The energy functional $E_{image}(\mathbf{v}(s))$ is defined more precisely as follows

$$E_{image} = \omega_{line}E_{line} + \omega_{border}E_{border} + \omega_{term}E_{term} \tag{4}$$

All the functionals in (4) represent the characteristics that the user defines. The main functions of each functional are:

- The functional E_{line} have minimums on dark or bright lines depending on the sign of ω_{line}.
- The functional E_{border} uses the gradient to identify borders.
- The functional E_{term} uses a discrete definition of curvature to identify corners.

All the mathematical expressions of the previous functional are explained in Kass [1] or Cohen [4].

The previous functional $E_{extern\_force}(\mathbf{v}(s))$ in (2) is used to interact with the model, i.e., the curve could find a wrong local minimum, then the user could define a point near the desired solution in order to attract the curve.

As explained, it is necessary to find a differential equation that guarantees a minimum in (1). The solution proposed by Kass is based on the Euler-Lagrange equation that is a differential equation that finds a local minimum for the energy functional (more details in Weinstock [8]). The Euler-Lagrange equation for (1) is expressed as follows

$$\frac{\partial E_{extern}}{\partial \mathbf{v}} - (\alpha\, \mathbf{v}'(s))' + (\beta\, \mathbf{v}''(s))'' = 0 \tag{5}$$

where the energy functional E_{extern} is defined as

$$E_{extern} = E_{image} + E_{extern\_force} \tag{6}$$

There is not an explicit solution for (5), but it can be solved through an iterative process. Kass proposed solving it by the gradient descent method that has the negative issue that supposes an initialization near the local minimum. In consequence, the model will need to set the initial points near the minimum. Therefore, the previous is defined by the following equation

$$\frac{\partial E_{extern}}{\partial \mathbf{v}} - (\alpha\, \mathbf{v}'(s))' + (\beta\, \mathbf{v}''(s))'' = -\frac{\partial \mathbf{v}(s)}{\partial t} \tag{7}$$

To get a final descriptor of the curve, it is necessary to translate (7) in a discrete space, then the final equation is expressed as

$$\mathbf{v}_i^t = \left(\mathbf{A} + \frac{1}{\tau}\mathbf{I}\right)^{-1} \left(\frac{1}{\tau}\mathbf{v}_i^{t-1} + \gamma\, \mathbf{f}_i^{t-1}\right) \tag{8}$$

where $\mathbf{f}_i^t = \frac{\partial E_{extern}}{\partial \mathbf{v}}$.

In (8) the matrix $\mathbf{A}$ is a pentadiagonal matrix that has desired properties to get its inverse [9]. The term τ is a representation of the discrete time and γ is a parameter that regulates the behavior of the term $\mathbf{f}_i^t$.

To conclude this section, the table 1 presents a summary of the advantages and disadvantages reported and others like finding concavities that will be explained in section 5.

ADVANTAGES	DISADVANTAGES
1. Fast	1. Define the value of each parameter. 2. Control points location near the desired object. 3. Does not find concavities.

Tabl. 1. Comparative table for the Kass model

4. Cohen model

As commented in section 2, the Kass model has the disadvantage of considering the initial curve near the desired local minimum. In 1991, Laurent Cohen [4] proposed a new expression for $\mathbf{f}_i^t$ in order to fix the problem originated by the descent gradient method and problems related to noise as well.

Laurent Cohen uses $\mathbf{F}_{extern}^{(g)}$ as the expression $\mathbf{f}_i^t$ in section 2. A new superscript *g* is added to the external force that means "general". In this model it is proposed $\mathbf{F}_{extern}^{(g)}$ to represent a more general force that includes two types of force: static force and dynamic force. The static force is the particular force, which does not vary and the dynamic force is adjusted. Cohen proposal arises because of Kass model incapacities to overcome difficulties by the fact of having a model evolving in the discrete time domain. If γ $\mathbf{f}_i^{i-1}$ is big, then curve $\mathbf{v}_i^t$ could go beyond the desired minimum. What could happen is that when force γ $\mathbf{f}_{extern}^g$ acts again, control point $\mathbf{v}_i$ tries to find the local minimum or, which is worst, it does not find the minimum and only internal force has an effect on it. What has to be done is to choose γ small enough to avoid oscillations; however, this causes an effect of slow advance which is also not desired. This expression must be used in (8) to avoid the problem of the gradient descent method commented before. Therefore, $\mathbf{F}_{extern}^{(g)}$ is suggested to be defined as follows

$$\mathbf{F}_{extern}^{(g)} = -\kappa_1 \mathbf{n}(s) + \kappa \frac{\nabla E_{extern}}{\left\| \nabla E_{extern} \right\|} \quad (9)$$

In (9), κ is chosen in order to minimize the effect of γ in (8) and κ_1 is a new parameter that controls the importance of $\mathbf{n}(s)$ that is the normal vector of the curve. The new expression in (9) for E_{extern} is a normalization and the nabla operator is the same expression of derivation in (8).

The normal vector has the particular benefit that it will conduct the curve to a desired minimum depending if the model is required to inflate or compress depending to the initial control points.

Due to the discrete mapping of the external force, it might happen that a minimum is reached for a non integer value and therefore it is not contained in the map of external forces $\mathbf{F}_{extern}^g$. To solve these mapping problems there are different approximation techniques such as zero-order interpolation, cubic convolution interpolation or bi-lineal interpolation [17]. This last method is the most utilized due to its good efficiency and approximation.

As it was done in the last section, table 2 resumes the advantages and disadvantages commented.

ADVANTAGES	DISADVANTAGES
1. Fast 2. Good behavior under noise conditions.	1. Define the value of each parameter. 2. Control points location defines the behavior of the model (inflation or compression). 3. Does not find concavities.

Tabl. 2. Comparative table for the Cohen model.

5. Xu model

In 1999, Chenyang Xu [5] considered an alternative solution for the external force $\mathbf{F}_{extern}^{(g)}$, which will be again used in substitution of $\mathbf{f}_i^t$ in (8). This time the design is intended to locate the control points for the desired object without restrictions of inflation or compression produced by the normal vector in the model of Cohen in (9). That means that no indications prior the location is necessary. Aside for the location of the control points, Xu used his design to deform the curve correctly on concavities.

As in the Cohen model, the model of Xu uses an alternative external force $\mathbf{F}_{extern}^{(g)}$ that has in this case the name of GVF (Gradient Vector Flow) force. The idea is similar to the proposition of Kass, although the goal is to generate a field that conducts the curve to the desired object with the characteristics discussed before. Therefore a vector field $\mathbf{v}_{GVF}$ must have high values near the borders and a constant field far from it. In consequence to the constant field, the problem of far location is solved. On the other side, the concavities are found as a direct consequence of the constant field as reported by Xu in [5]. The equation used by Xu is the following.

$$E_{GVF} = \int \mu \left(u_x^2 + u_y^2 + v_x^2 + v_y^2\right) + |\nabla f|^2 \left|v_{GVF} \quad \nabla f\right|^2 dxdy \tag{10}$$

where f is a border map that generates a high output near the borders of the object, (u, v) are components of the vector field $\mathbf{v}_{GVF}$ and in (10) are differentiate respect to the spatial coordinates. There is also a parameter μ that regulates the importance of the constant field.

Equation (10) represents a problem where it is necessary to find a field $\mathbf{v}_{GVF}$ that will generate a local minimum for the energy functional E_{GVF}. The term $|\nabla f|^2 |\mathbf{v}_{GVF} - \nabla f|^2$ in (10) generates a minimum near the borders of the desired object and the other term $\left(u_x^2 + u_y^2 + v_x^2 + v_y^2\right)$ has a minimum when a constant value is found. A similar expression is

found in the optical flow definition [10]. Fig. 1 represents the GVF field for a picture that consists of a black line square in a white background. The vectors (observed in Fig. 1 as blue points of different dimensions) represent the direction and magnitude of the GVF field that will guide the curve to the desired object.

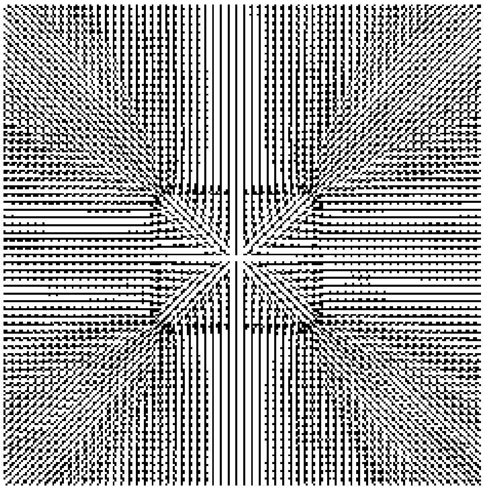

Fig. 2. GVF field example.

The comparative table for the Xu model is shown in table 3 where the principal disadvantage that was not commented is that it is slower than the other two models. This is because the GVF model must be calculated.

ADVANTAGES	DISADVANTAGES
1. Control points location far the desired object. 2. Find concavities	1. Define the value of each parameter. 2. Slow

Tabl. 3. Comparative Table For The Xu Model.

6. Design of the experiment

In the three comparative tables discussed, one can find that a common disadvantage is the definition of the parameters. Rousselle [7] suggests solving this problem through the design of experiments that ensure the best parameter values through a defined process of experimentation. Nevertheless, the output of Rousselle´s experiment requires a large number of samples because this is defined as a quantitative note given by an experimenter. In this report, another way to solve this problem is suggested using a more precise output that will avoid doing many experiments and will ensure adequate values for the parameters, although not the optimums.

The goal of the experiment is to find good parameters for each model studied in this project. Good means that an optimal result is not guaranteed.

Each model has a different number of parameters to be studied although in this experiment only three parameters will be considered. In the model of Kass there are only three parameters (α, β, γ), the model of Cohen has five $(\alpha, \beta, \kappa_1, \kappa, \gamma)$ and the model of Xu has four $(\alpha, \beta, \mu, \gamma)$. Nevertheless, in the case of the model of Cohen κ and γ are correlated and in consequence the first could be not considered. On the other side, κ_1 must be inferior to κ in order to avoid an excessive influence of the normal vector, therefore κ_1 is fixed to the low level of κ that will be defined below. At last, Xu suggests a value for μ and also demonstrates that in general small values for this parameter guarantee a relative fast model that converges. Therefore, only three parameters are considered for each model.

Each parameter is considered as a factor with three levels; low level, medium level and high level. The highest level is defined in order to avoid problems as oscillation, excessive smoothness or compression of the model, characteristics that have been studied. Once the high level is defined, the other two are uniformly separated knowing that each parameter is lineal and given as a restriction zero as the lowest level. Table 4 shows the values elected for each parameter.

	α	β	γ
Low	0.05	0	.15
Medium	0.30	0.5	1.15
High	0.55	1	2.15

Tabl. 4. Levels for the parameters in the three models.

In this experiment the output is defined as an interaction of the parameters studied above and is given in terms of a percentage that represents the proportion of related pixels between a desired object and the final curve that is used for the experiment using one of the 27 possible combinations in table 4.

This kind of output is useful in cases where the model will be used for specific situations or for related objects under similar conditions of intensities; otherwise, the external forces could change drastically. An example like the one in Fig. 2, where the red line represents the initial control points, is used for the experiment and the result of this experiment using the model of Kass is shown in table 5 where the sub index number of each parameter represents the low, medium or high level from the lowest number to the highest.

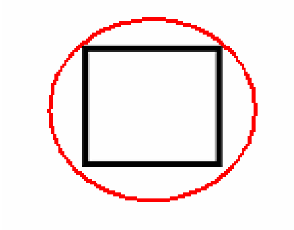

Fig. 3. Experiment example.

		β_1	β_2	β_3
γ_1	α_1	0	0	0
	α_2	0	0	0
	α_3	0	0	0
γ_2	α_1	65.2174	95.1220	95.1220
	α_2	94.8718	95	95.1220
	α_3	94.8718	94.8718	94.84718
γ_3	α_1	75.6410	95.1220	95.1220
	α_2	95.0617	95.1220	95.1220
	α_3	94.9367	95.1220	95.0617

Tabl. 5. Experimental results for the example in Figure 2 using the Kass Model.

7. Real example

An example on this investigation using real gray scale images is needed to ensure the methods proposed. Fig. 3 shows a real example where the red line represents the initial curve. This curve is located manually by the user that is looking to find the borders and corners of the box. Using the parameter values of a simple rectangular picture for the Cohen and Xu models the final results are shown in Fig. 4 and Fig. 5 respectively. Both figures demonstrate a general good behavior although there are zones where the model is not exact but in this is not the fault of the parameter values but of the external force definition. Nevertheless, the objective of the good behavior of the parameters is shown.

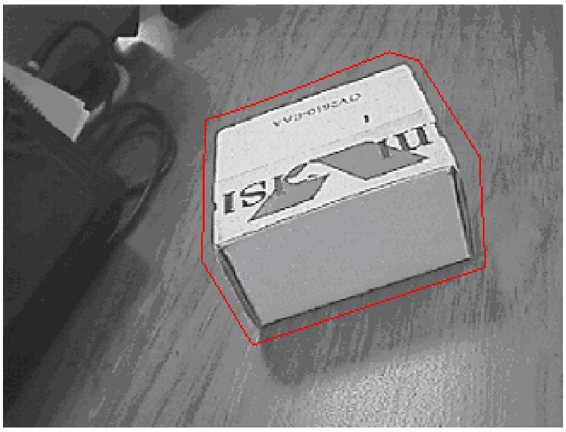

Fig. 4. A gray scale image with an initial curve around the desired object.

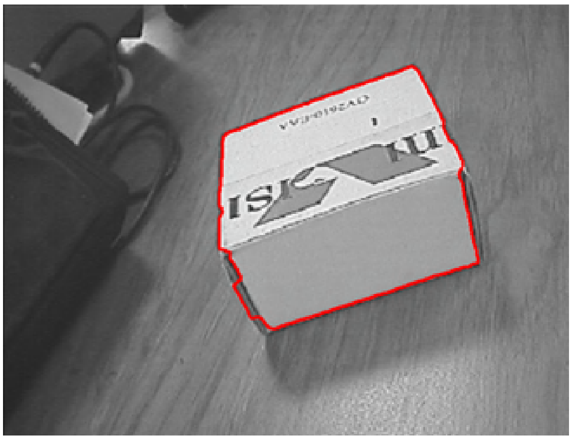

Fig. 5. Final result using the Cohen model.

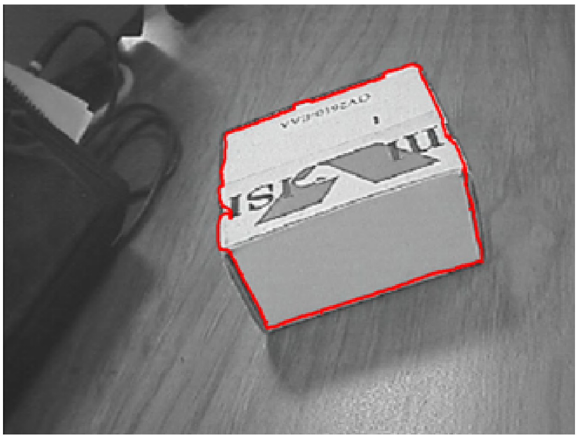

Fig. 6. Final result using the Xu model.

8. Conclusions

Active contour models represent an alternative for segmentation of images with the ability of having the user choosing an area of interest for segmentation and not leaving the final solution to a low level process [15].

This document presents a comparison of three active parametric models and an explanation of each one. This kind of comparative studies are useful to identify specific and strong models for certain applications. This comparison is not given by any previous paper.

An alternative experiment design for the three models studied is made with good results as shown in the real image in Fig. 4 and Fig. 5. These experiments might contain as many factors as required. This project does not consider the convergence time due to the fact that it is more interesting to observe the behavior of the model when it had detected contours, and with this it was possible to define a threshold to truncate the number of iterations; however, without finding the minimum forces to realize all the iterations and to correctly define external forces and utilize the adequate model. This experiment design technique could be extended to other cases when convergence time is an important factor of observation.

In the performed tests the threshold had different variations for different environments in the Xu model but not in the Cohen model. Different test were performed with a chosen threshold in other examples and there were good results, if control points are not located close to other minimums because these thresholds will bring the curve to false minimums. This problem is solved by the user interaction or variations when defining external forces.

The purpose is to show that the user has the ability to use the prior knowledge. An example of this is better explained in Fig. 6 where the result of Fig. 4 is compared with the Canny operator that finds all the discontinuities over certain range in the image although the user has not capabilities to suggest which discontinuities are the desired.

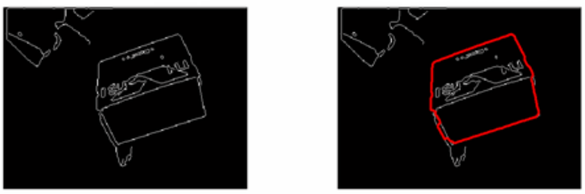

Fig. 7. Canny operator vs. Active model.

Applications can be used in cases where detection of similar objects is made under constant image conditions like brightness or cam position.

There is work done on parametric active contour models called b-snakes or b-spline snakes [3] based on b-spline theory [11-12]. These models use few parameters and have an implicit smoothing term, which facilitates its implementation. Other models which are subject of study are the geodesic active contour models [13] that belong to the family of geometric active contour models, which have the ability of changing their topology. New models are searched for to solve the problems due to snaxels which are slow convergence, difficulty for determining the parameter values, curve description by a finite set of disconnected points, inaccurate high-order derivatives in environments with noise for discrete curves.

The implementation of a model to overcome all these problems is the next requiring step, and the theory developed in this work gives the foundations to analyze other models and the experiment design technique to be used in other models.

Commercial applications of the active contour models suggested are in the field of medicine (Identification of brain zones of interest for physicians, segmentation of brain zone from bone zone [16], segmentation of carotid arteries on ultrasonic images for measurement of damages), in the field of object recognition (Object Tracking [14], Identification of buildings or rivers in aerial images, Road identification for artificial vision in automobiles, forest fire detection), and the field of video editing (object extraction for color changing). The main purpose is utilizing active contour models in tasks where there is a previous definition of what is desired to be found. This kind of definition is known as a priori knowledge [2].

With the experimentation design technique described, active contour model description and references, it is possible to develop applications such as those previously commented or to develop a similar procedure as the one described here from other current models such as the b-splines or the geometric model.

Acknowledgment
We would like to thank Dr. Chenyang Xu for his permission to use some of his functions in MATLAB for the application of the models, as well as Dr. Araceli Ramírez for the AFM image of figure 1*.

References

[1] M.Kass, A. Witkin, and D. Terzopoulos, “Snakes: active contour models,” International Journal on Computer Vision, vol.1, 1987, pp. 321-331.
[2] A. Blake and M. Isard, Active Contours, Great Britain: Springer-Verlag, 2000.
[3] P. Brigger, J. Hoeg and M. Unser, “B-Spline Snakes: A Flexible Tool for Parametric Contour Detection,” IEEE Transactions on Image Processing, vol. 9, September 2000, pp. 1484-1496.
[4] L. D. Cohen, “On active contour models and balloons,” CVGIP: Image Understanding, vol. 53, March 1991, pp. 211-218.

[5] C. Xu and J. L. Prince, “Snakes, shapes, and gradient vector flow,” IEEE Transactions on Image Processing, vol. 7, 1998, pp. 359-369.
[6] M. Jacob, T. Blu and M. Unser, “Efficient Energies and Algorithms for Parametric Snakes,” IEEE Transactions on Image Processing, vol. 13, September 2004, pp. 1231-1244.
[7] J. J. Rouselle, N. Vincent, Design of experiments to set active contours, Laboratoire d´Informatique (LI), Université Francois Rabelais de Tours, 2002.
[8] R. Weinstock, Calculus of Variations, New York: Dover Publications INC., 1974
[9] A. Benson and D. J. Evans, “A normalized algorithm for the Solution of Positive Definite Symmetric Quindiagonal Systems of Linear Equations,” ACM Transactions on Mathematical Software, vol. 3, 1977, pp. 96-103.
[10] B. K. P. Horn and B. G. Schunck, “Determining optical flow,” Artificial Intelligence, vol. 17, 1981, pp. 185-203.
[11] M. Unser, A. Aldroubi, Murray Eden, “B-spline signal processing Part I: Theory,” IEEE Transactions on Signal Processing, vol. 41, February 1993, pp. 821-833.
[12] M. Unser, A. Aldroubi, Murray Eden, “B-Spline Signal Processing Part II: Efficient Design and Applications,” IEEE Transactions on Signal Processing, vol. 41, 1993, pp. 834-848.
[13] V. Caselles, R. Kimmel, G. Shapiro, “Geodesic Active Contours,” Proceedings of the Fifth International Conference on Computer Vision, 1995, pp. 694-699.
[14] R. K. Raman, Active Contour Models for Object Tracking. Dissertation, St. Edmunds College, England, 2003.
[15] J. P. Ivins, Active Region Models. Master Degree Dissertation, University of Sheffield, England, 1996.
[16] C. Xu, Deformable Models with Application to Human Cerebral Cortex Reconstruction from Magnetic Resonance Images, Doctoral Dissertation, Johns Hopkins University, Baltimore, 1999.
[17] D. Williams, M. Shah, “A Fast Algorithm for Active Contour and Curvature Estimation,” CVGIP: Image Understanding, vol. 55, January 1992, pp. 14-26.
[18] R. C. Gonzalez, R. E. Woods, Digital Image Processing. New Jersey: Prentice Hall, 2001.